

Optical characteristics of gold nanoparticle-doped multilayer thin film

Hongbo Liao

Department of Physics, Beijing Normal University, Beijing, 100875, China and Department of Physics, Hong Kong University of Science and Technology, Clear Water Bay, Kowloon, Hong Kong

Weixin Lu, Shengwen Yu, Weijia Wen, and George K. L. Wong

Department of Physics, Hong Kong University of Science and Technology, Clear Water Bay, Kowloon, Hong Kong

Received November 23, 2004; revised manuscript received March 17, 2005; accepted March 28, 2005

A variety of surface plasmon resonance (SPR) peaks of gold nanoparticles was detected in the wavelength range between the SPR peak of Au/SiO₂ (~535 nm) and Au/TiO₂ (~655 nm) with the parameter x in the triple-component composite films, (SiO₂)_{1-x}/Au/(TiO₂)_x. Based on the spectrum of the dielectric constant of Au and the location of the SPR peaks, the effective refractive index n_{eff} of these composite films was found to be almost equal to $n_{\text{SiO}_2} \cdot (1-x) + n_{\text{TiO}_2} \cdot x$. These composite films can be used as optical filters owing to their high damage threshold value (>6.5 MW/cm²). Their potential applications in nonlinear optical devices are due to their larger third-order nonlinear susceptibilities, $\chi^{(3)}$, which were measured by the degenerate four-wave-mixing method at a laser wavelength of 532 nm. The $\chi^{(3)}$ value reached 2.6×10^{-6} esu. © 2005 Optical Society of America

OCIS codes: 190.2640, 190.4380, 160.4760.

1. INTRODUCTION

Materials with large third-order optical nonlinearity and fast response time are essential for future optical device applications.^{1,2} In the past decade, it was found that composites consisting of metal nanoparticles (such as Au, Ag, and Cu),^{3,4} embedded in a dielectric matrix were among the most attractive candidates for such applications owing to their very large nonlinear susceptibility $\chi^{(3)}$, which was known to stem from the enhancement of the local field factor near the surface plasmon resonance (SPR).^{5,6} At the limit of low metal concentration, $\chi^{(3)}$ was proportional to the fourth power of the local field factor. That is, a larger value of the local field factor was very important for improving the nonlinearity of such a composite.

The local field factor f takes the form of $f = 3\epsilon_d / (\epsilon_m + 2\epsilon_d)$, where $\epsilon_m = \epsilon_1 + i\epsilon_2$ and ϵ_d are the dielectric constant of the metal and the dielectric matrix, respectively. Around the SPR, f can be reduced to $3\epsilon_d / i\epsilon_2$. Obviously, near the SPR peak, a matrix with a larger dielectric constant could make the composite gain a larger value of f and, in the meantime, the SPR peak should also exhibit a shift due to the energy dependence of the dielectric constant of the metal particle.⁷ Therefore, when compared with commonly used metal-doped glasses, the composites with metal particles embedded in a matrix with a large refractive index, such as TiO₂ (Ref. 8), ZnO (Ref. 9), or BaTiO₃ (Ref. 10), usually have larger optical nonlinearities near their individual SPR peaks. However, these kinds of matrices are easily crystallized during thermal treatment, and then their small metal particles can join together to grow. This may result in a decrease of their nonlinearity owing to the formation of very large metal particles, because the size-dependent $\chi^{(3)}$ could have a

maximum value at an optimal metal-particle size (~30 nm).¹¹ Hence, it has been important to find a way to control the metal-particle size and the size distribution in such composites in order to guarantee a large third-order nonlinearity. Multilayer structures were shown to be able to control the size distribution of the metal particles to some extent, because the layer of the dielectric matrix might prevent the movement of the metal particles from gathering.

2. EXPERIMENTS

(SiO₂)_{1-x}-Au-(TiO₂)_x multilayer composite films were prepared on the fuse quartz substrates in a three-target magnetron sputtering system with computer-controlled target switching capability (Denton SJ/24 LL). Here the parameter x represents the volume percentage of TiO₂ films, and $(1-x)$ represents that of SiO₂ films. Some of the deposition parameters are listed in Table 1. The Au target was controlled by an rf power supply to have a lower deposition rate, whereas the TiO₂ film was obtained by introducing the oxygen atmosphere (with an Ar:O₂ ratio of approximately 9:1) into the chamber during the sputtering of Ti. The refractive index of the TiO₂ film obtained in our experiment was ~2.4 at the wavelength of 632 nm. Prior to the multilayer deposition, the growth rate of each component was calibrated by separately sputtering the three targets under the same deposition conditions. The results are listed in column 3 of Table 1. Two sets of (SiO₂)_{1-x}-Au-(TiO₂)_x samples with an Au layer thickness of ~4 nm were prepared for our investigation. One set of samples had layers of SiO₂ and TiO₂ with the same thickness ($x=0.5$) of about 15 nm. The other was prepared

Table 1. Experimental Parameters Used in the Preparation of SiO₂/Au/TiO₂ Composites

Target	Power Supply	Deposition Rate (Å/s)	Thickness of the Layer (nm)	Number of Layers	Ratio of Ar:O ₂
SiO ₂	rf	0.55	15	8	9:1
Au	rf	0.64	4	15	
Ti(TiO ₂)	dc	0.22	15	8	

by changing the film thickness of SiO₂ and TiO₂ but leaving their total thickness unchanged in order to obtain composite films with the same Au concentration but a different value of x . Most of our experiments were done by using the former set of samples (noted as SiO₂/Au/TiO₂ in the following text).

The thermal treatment of the as-grown multilayer films was carried out in a high-temperature furnace. The crystallinity of the multilayer films was investigated by the x-ray diffraction (XRD) method (model: Philips PW1830). Also, the cross-sectional microstructures of the SiO₂/Au/TiO₂ multilayer films were investigated by transmission electron microscopy (TEM) (model: Philips CM120). The linear optical absorption spectra of these films were measured by a UV-visible (UV-VIS) spectrophotometer (Perkin-Elmer, λ 20) in the range of 300–1000 nm. The third-order nonlinear susceptibility $\chi^{(3)}$ was measured at 532 nm using an Nd:YAG laser (Q switched and mode locked) and employing a standard backward degenerate four-wave-mixing (DFWM) scheme. The laser had a pulse duration of 70 ps, a repeat rate of 500 Hz, and a maximum peak power of ~ 6.5 MW/cm². A high-sensitivity photodiode and a lock-in amplifier were used to detect the nonlinear signals. The value of the effective $\chi^{(3)}$ was measured relative to CS₂, a reference medium that has $\chi^{(3)} = 2 \times 10^{-12}$ esu in the picosecond time scale, by using the following equation¹²:

$$\chi^{(3)} = \chi_{CS_2}^{(3)} \left(\frac{I_s}{I_{CS_2}} \right)^{1/2} \frac{n_s^2 L_{CS_2} \ln(1/T)}{n_{CS_2}^2 L_s (1-T)\sqrt{T}}, \quad (1)$$

where I_s and I_{CS_2} are the intensity of the conjugate signal; n_s and n_{CS_2} are the respective refractive indices; L_s and L_{CS_2} are the thickness of the SiO₂-Au-TiO₂ composite films and the CS₂, respectively; and T is the transmissivity of the SiO₂-Au-TiO₂ films at a given laser wavelength.

3. RESULTS AND DISCUSSIONS

After the heat treatment, the SiO₂-Au-TiO₂ films were purple in color owing to the formation of the Au particles. Also, the color of the (SiO₂)_{1-x}-Au-(TiO₂)_x films changed from ruby to blue with an increase in the value of x from 0 to 1. The crystallization of some selected SiO₂-Au-TiO₂ films measured by XRD methods is shown in Fig. 1. Obviously, the Au nanoparticles were well crystallized under the experimental thermal annealing condition. In comparing the peak intensity of the Au(111) and Au(200), we know that the Au crystallites have a texture characteristic along the (111) direction. It

should be noted that the TiO₂ did not crystallize when the annealing temperature was set at 950 °C [Fig. 1(a) and 1(b)], while TiO₂ crystallites with rutile structures appeared when the temperature increased to 1050 °C [Fig. 1(c)]. The peak intensity of TiO₂(110) also became higher with an increase in the annealing duration [Fig. 1(d)] due to the growth of the TiO₂ particles. The broad peak around $2\theta = 22^\circ$ indicated that the SiO₂ films were always amorphous even after being annealed at 1050 °C for 12 h.

Selected cross-sectional TEM pictures of the SiO₂-Au-TiO₂ film with the same dimensional scale are shown in Fig. 2. As seen in Fig. 2(a), the as-grown films had a very good multilayer structure, where the layers with the same color as the substrate are SiO₂ and those

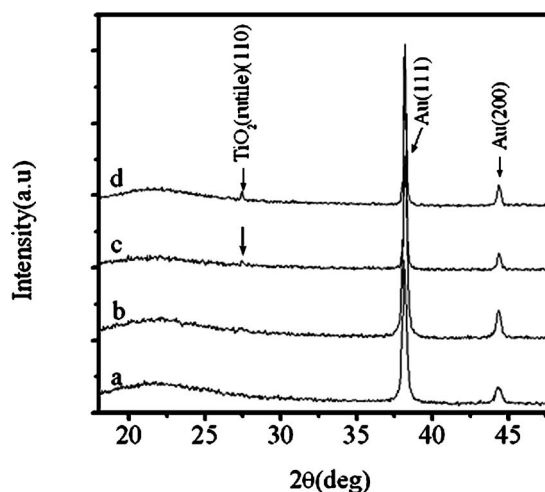


Fig. 1. The x-ray diffraction data of SiO₂/Au/TiO₂ composites. The sample was annealed at (a) 950 °C for 1 h, (b) 950 °C for 10 h, (c) 1050 °C for 2 h, and (d) 1050 °C for 12 h.

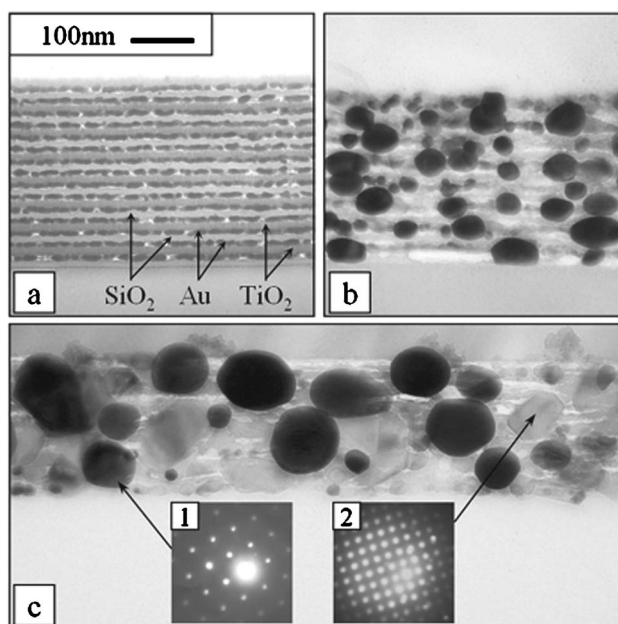


Fig. 2. Selected cross-sectional TEM pictures of SiO₂/Au/TiO₂ composites. (a) As-grown films, the sample annealed at (b) 950 °C for 1 h, (c) 1050 °C for 12 h. The inset is the diffraction pattern of: (1) Au particles; (2) rutile TiO₂.

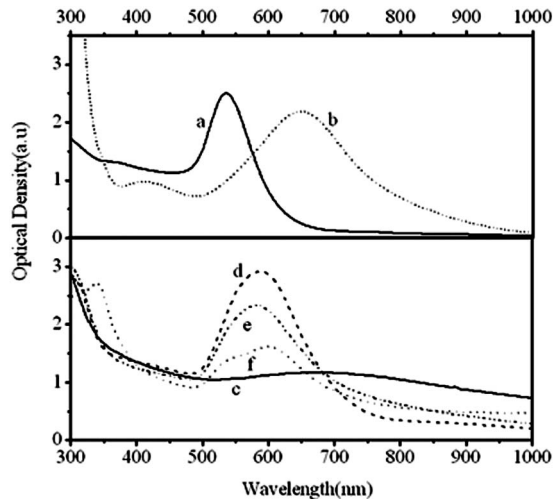


Fig. 3. UV-VIS spectra of $\text{SiO}_2/\text{Au}/\text{TiO}_2$ composites. (a) pure Au/SiO_2 films, (b) pure Au/TiO_2 ; $\text{SiO}_2/\text{Au}/\text{TiO}_2$ composite films; (c) as-grown films, annealed at (d) 950°C for 1 h, (e) 950°C for 10 h, and (f) 1050°C for 12 h.

with a deep gray color are TiO_2 . Before annealing, very small Au particles [the dark curves in Fig. 2(a)] were sandwiched by SiO_2 and TiO_2 and were almost connected with each other to form a uniform film. However, after being annealed at 950°C for 1 h, the small Au particles aggregated together and became much bigger [Fig. 2(b)]. It should be noted that although the morphology of the multilayer structure remains in the annealed films, the repeat period changes. By simply comparing Figs. 2(b) and 2(a), it is easy to see that there are only eight layers of Au after the annealing instead of 15 layers before the annealing. This may be because the Au atoms go through the TiO_2 layer but are confined by the SiO_2 layers when annealed at 950°C . The reason that SiO_2 films have a stronger confinement effect than TiO_2 on the movement of Au particles is probably because SiO_2 films have a lower porosity and are not easy to crystallize. However, with a further increase of the annealing temperature to 1050°C , the confinement effect of the SiO_2 layers disappears, and the morphology of the multilayer structure of $\text{SiO}_2\text{-Au-TiO}_2$ films is lost. When the electron beam is focused on individual crystallites, we see that two types of diffraction patterns are obtained, and this result reveals that the two kinds of particles are small single crystals but with different lattice constants and symmetries [insets 1 and 2 in Fig. 2(c)]. When combined with the XRD result shown in Fig. 1, these results indicate that the gray particles are TiO_2 crystallites.

The UV-VIS spectra of the $\text{SiO}_2\text{-Au-TiO}_2$ films are shown in Fig. 3. The a and b curves in Fig. 3 are the absorption spectra of the pure Au-SiO_2 and Au-TiO_2 multilayer films, respectively, which were prepared in the same sputtering system and annealed at 950°C for 1 h. It is clear that the SPR peak of the pure Au-SiO_2 (typically located around 535 nm) was much narrower than that of Au-TiO_2 (located around 655 nm) owing to the more uniform distribution of the Au particles in the Au-SiO_2 films. The $\text{SiO}_2\text{-Au-TiO}_2$ multilayer films annealed at 950°C had SPR peaks around 585 nm (curves d and e in Fig. 3) while the as-grown films that were brown

in color usually had no special SPR peaks (as shown in curve c in Fig. 3). With an increase in the annealing temperature to 1050°C , the SPR peak tended to split into two peaks: one close to that of Au-SiO_2 and the other approaching to that of Au-TiO_2 (curve f of Fig. 3). In the meantime, the peak intensity also decreased owing to the light scattering caused by the very large Au particles formed during the higher temperature annealing. As seen in Fig. 3, the SPR peaks in the $\text{SiO}_2\text{-Au-TiO}_2$ films were also narrower than those of the pure Au-TiO_2 films. To some extent, this reveals that the former film should have a more uniform particle distribution, owing to the confinement effect of SiO_2 layers.

The dependence of the SPR peaks of $(\text{SiO}_2)_{1-x}\text{-Au-(TiO}_2)_x$ films on the parameter x is shown in the inset of Fig. 4. The samples used here were of the same Au concentration and were all annealed at 950°C . It is clear that the SPR peaks shifted from 535 to 655 nm when x was varied from 0 to 1 (the inset in Fig. 4). On the basis of the wavelength of the SPR peaks and the spectrum of the dielectric constant of Au, we may calculate the effective refractive index n_{eff} of the $(\text{SiO}_2)_{1-x}\text{-Au-(TiO}_2)_x$ films. The result is plotted in Fig. 4 versus the parameter x . The dashed line shown in Fig. 4 was obtained by using the equation $n_{\text{eff}} = n_{\text{SiO}_2} \cdot (1-x) + n_{\text{TiO}_2} \cdot x$, where $n_{\text{SiO}_2} = 1.46$ and $n_{\text{TiO}_2} = 2.4$ are the refractive indices of pure SiO_2 and TiO_2 films, respectively, prepared in our sputtering system. As seen from Fig. 4, the value of n_{eff} measured in our experiment was very close to this linear equation. Thus a way to change the location of the SPR peak of such composite films is to use multimatrix materials.

The third-order nonlinear susceptibilities, $\chi^{(3)}$, measured by DFWM and the size of Au particles measured by XRD of the annealed $\text{SiO}_2\text{-Au-TiO}_2$ samples are listed in Table 2. As seen in Table 2, the film annealed at 950°C for 1 h had an $\chi^{(3)}$ value of about 2.6×10^{-6} esu, which was very close to that of the Au-SiO_2 composite film and was ~ 1 order of magnitude larger than that of Au-TiO_2 .

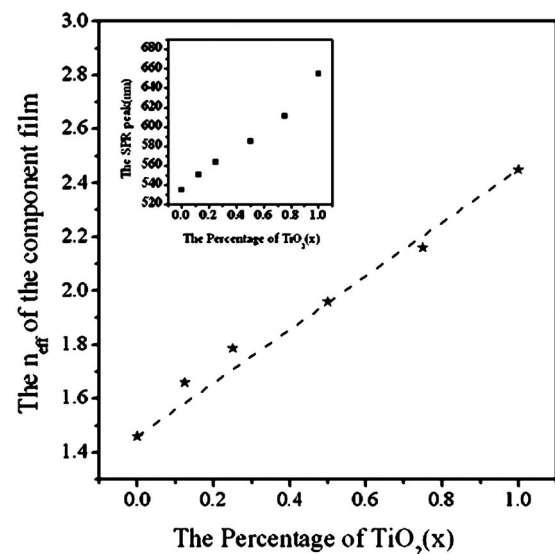


Fig. 4. Dependence of the effective refractive index n_{eff} of $(\text{SiO}_2)_{1-x}/\text{Au}/(\text{TiO}_2)_x$ composite films on the parameter x . The dependence of the wavelength of their SPR peaks on the parameter x is shown in the inset.

Table 2. Third-Order Nonlinear Susceptibilities, $\chi^{(3)}$, of SiO₂/Au/TiO₂ Composites

Sample	1	2	3	4	5
Annealing condition	950 °C 1 h	950 °C 2 h	950 °C 10 h	1050 °C 2 h	1050 °C 12 h
Particle size of Au (nm)	27.7	35.4	38.7	44.9	57.4
$\chi^{(3)}$ (10 ⁻⁷ esu)	26	22	18	9.4	–

With an increase in the annealing temperature, the value of $\chi^{(3)}$ decreases owing to the growth of the gold particles. The $\chi^{(3)}$ value of the sample annealed at 1050 °C for 12 h could hardly be measured because of the serious light scattering caused by the very large Au particles. That is, the triple-component SiO₂-Au-TiO₂ film maintained the large third-order nonlinearity of the pure Au-SiO₂ composite film at the wavelength of 532 nm. It is known that the stronger the light absorption is, the larger value of $\chi^{(3)}$ is. Therefore, based on its absorption spectrum, the SiO₂-Au-TiO₂ film should also achieve a large $\chi^{(3)}$ in a wide range of wavelengths, at least between the SPR peaks of Au-SiO₂ and Au-TiO₂.

4. CONCLUSIONS

In summary, gold nanoparticles were found in the triple-component (SiO₂)_{1-x}-Au-(TiO₂)_x composite films after thermal annealing. These films had multilayer structures, with the Au layer being sandwiched between one layer of SiO₂ and another layer of TiO₂. The SPR peaks induced by the gold nanoparticles doped in such thin films were found to vary with the parameter x in a wavelength range between the SPR peak of Au-SiO₂ (~535 nm) and that of Au-TiO₂ (~655 nm). On the basis of the spectrum of the dielectric constant of metal Au and the location of the SPR peaks, the effective refractive index n_{eff} of these composite films was found to be almost equal to $n_{\text{SiO}_2} \cdot (1-x) + n_{\text{TiO}_2} \cdot x$. Their third-order nonlinear susceptibility, $\chi^{(3)}$, measured by DFWM method at a laser wavelength of 532 nm, can reach a value of 2.6×10^{-6} esu, which is com-

parable with that of the Au-SiO₂ films. The SiO₂-Au-TiO₂ film might also gain a large $\chi^{(3)}$ in a wavelength range between the SPR peaks of Au-SiO₂ (about 535 nm) and Au-TiO₂ (about 655 nm) owing to its strong absorption in this wavelength range.

ACKNOWLEDGMENT

The authors thank Hong Kong RGC (project No. 603603) for their support of this work. W. Wen is the corresponding author and can be reached at phwen@ust.hk.

REFERENCES

1. Y. R. Shen, *The Principles of Nonlinear Optics* (Wiley, 1984).
2. J. I. Sakai, *Phase Conjugate Optics* (McGraw-Hill, 1994).
3. I. Tanahashi, Y. Manabe, T. Tohda, S. Sasaki, and A. Nakanura, "Optical nonlinearities of Au/SiO₂ composite thin films prepared by a sputtering method," *J. Appl. Phys.* **79**, 1224–1249 (1996).
4. K. Uchida, S. Kaneko, S. Omi, C. Hata, H. Tanji, Y. Asahara, and A. Nakanura, "Optical nonlinearities of a high concentration of small metal particles dispersed in glass: copper and silver particles," *J. Opt. Soc. Am. B* **11**, 1236–1243 (1994).
5. D. Ricard, P. Roussignol, and C. Flytzanis, "Surface-mediated enhancement of optical phase conjugation in metal colloids," *Opt. Lett.* **10**, 511–514 (1985).
6. E. Wolf, ed., *Progress in Optics XXIX* (Elsevier, 1991).
7. U. Kreibig and M. Vollmer, *Optical Properties of Metal Clusters* (Springer-Verlag, 1995), pp. 20–24.
8. H. Liao, R. Xiao, H. Wang, K. Wong, and G. K. L. Wong, "Large third-order optical nonlinearity in Au:TiO₂ composite films measured on a femtosecond time scale," *Appl. Phys. Lett.* **72**, 1817–1819 (1998).
9. H. Liao, W. Wen, G. K. L. Wong, and G. Yang, "Optical nonlinearity of nanocrystalline Au/ZnO composite films," *Opt. Lett.* **28**, 1790–1792 (2003).
10. G. Yang, W. Wang, Y. Zhou, Y. Lu, G. Yang, and Z. Chen, "Linear and nonlinear optical properties of Ag nanoclusters/BaTiO₃ composite films," *Appl. Phys. Lett.* **81**, 3969–3971 (2002).
11. H. B. Liao, W. Wen, and G. K. L. Wong, "Preparation and optical characterization of Au/SiO₂ composite films with multilayer structure," *J. Appl. Phys.* **93**, 4485–4488 (2003).
12. R. L. Sutherland, *Handbook of Nonlinear Optics* (Marcel Dekker, 1996).